J. Condensed Matter Nucl. Sci. 24 (2017) 301–311

Research Article

Controlled Electron Capture: Enhanced Stimulation and Calorimetry Methods

Francis Tanzella*
SRI International, Menlo Park, CA, USA

Robert Godes, Rogelio Herrera and Cedric Eveleigh
Brillouin Energy Corporation, Berkeley, CA, USA

Abstract

The Controlled Electron Capture (CEC) method has been extended to use faster rise and fall time pulses, hydrogen isotope gas based systems at temperatures up to 650°C, and more precise and accurate calorimetry relative to results presented earlier. Our isoperibolic (IPB) cell/calorimeter is operated as an isothermal compensation type calorimeter. Potential sources of error in this system are discussed as well the methods used to minimize them. In power compensation mode the cell is held at a constant temperature using a heater power feedback system and constant power pulses or DC power steps are added to the system, resulting in a reduction of heater power. The relationship between this heater power reduction and DC power passed along the reactor core yields a calibration curve at different temperatures that allows us to evaluate how much output power increased during a given stimulation pulse. The IPB cell/calorimeter was stimulated by commanding different pulse widths at constant amplitude with the pulse power held constant by appropriately varying the pulse repetition rate. At 250–300°C the ratio of output power increase to input pulse power varied from 1.0 to over 2.0 depending on the pulse width at constant input power. That ratio was always 1.0 at all pulse widths attempted at 600°C. These results have been seen tens of times. The amount of excess power was also dependent on the composition of the gas and the metal alloy coatings on the core. The outer layer of the core was always pure Ni. The composition of a multilayer metal–dielectric metal coated core was chosen to allow for reasonable hydrogen solubility and mobility at 300°C. The results of various experiments are discussed Importantly these results presented here ignore the heater power necessary to maintain temperature and the losses in the pulse generator, which can be several times greater than either the stimulation power or power gain.

Keywords: Controlled electron capture, Hydrogen, Isoperibolic, Nickel, Power compensation

---

[*] E-mail: francis.tanzella@sri.com.

1. Introduction

Since August 2012, SRI International (SRI) has been performing tests on two different versions of Brillouin Energy Corp.'s low-energy nuclear reactors (LENR) [1]. We have operated these reactors independently in an attempt to verify results that Brillouin has found with these reactors and others like them. We have also monitored and advised Brillouin on the results from reactors operated by Brillouin in their own laboratory. This report documents the results obtained by studies in SRI's laboratory, as well as verification and validation of results obtained in Brillouin's laboratory over the past nine months. Brillouin has indicated that it has designed the control systems in its reactors to drive the underlying physics of LENR, as described in its Controlled Electron Capture Reaction (CECR) hypothesis [2]. The CECR hypothesis explains how scientists at Brillouin believe their reactors generate controlled LENR reaction heat. Our study did not attempt to prove or disprove Brillouin's CECR hypothesis.

The systems tested and described in this report consist of three parts — cores, reactors, and calorimeters. The cores are the reactive components of the system. The reactors provide the environment and stimulation that causes the cores to produce reaction heat. The calorimeter is used to measure the thermal efficiency and absolute heat produced by the core-reactor system. The calorimeter was designed by both SRI and Brillouin personnel to be perfectly matched to the reactor. The results from two of these reactors are described in this report.

SRI has brought over 75 person-years of calorimeter design, operation, and analysis experience to this process. We have used our expertise in LENR calorimetry to validate the results summarized herein. Brillouin's system design utilizes compensation calorimetry, in which the core and reference temperatures are held constant by varying the input heater power while applying different types of stimulation that also input power to the reactor/calorimeter.

2. Experiment

2.1. Design

The cores consist of a metal substrate, which in some configurations includes a heater and thermocouple with several spray-coated layers. Generally, these coatings alternate between a hydrogen-absorbing metal and an insulating ceramic. One example is shown in Fig. 1. Other designs may have more or fewer layers. All of the layers are porous, allowing the gas(es) in the reactor chamber access to all coatings. There is a heater and thermocouple in the center of the core. The power to the heater is measured directly from the voltage and current supplied by the direct current (DC) power supply.

A photograph of the reactor/calorimeter system is shown in Fig. 2. The system is contained in an acrylic container filled with argon gas to minimize the probability of a hydrogen–oxygen reaction from any H_2 that might leak from the system. A schematic diagram of the reactor/calorimeter system is shown in Fig. 3. In a traditional isoperibolic calorimeter, the reactor temperature is distributed along a massive thermal block (inner block) surrounded completely

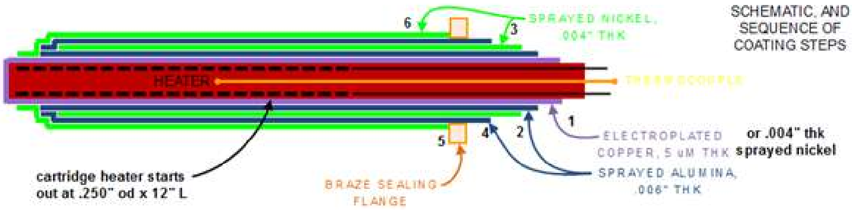

Figure 1. Example of Brillouin's fourth-generation hydrogen hot tube cores.

Figure 2. Photograph of the reactor/calorimeter system.

by a thick insulating layer, which itself is surrounded by another thermally conductive metal mass (outer block). This latter block is kept at a constant reference temperature.

Referring to the labeled parts of Fig. 3, the core (4) is centered in and insulated from a metal sheath (1). This core/sheath combination, together with the electrical connections (15), comprises the reactor. An annular copper or stainless steel block (3) is in intimate contact with the reactor sheath and contains a thermowell (2) and thermocouples and acts as the inner block. This copper block is surrounded by an annular ceramic insulator (14). Surrounding this insulator is an aluminum shell (5) with a thermowell and thermocouples. This shell, kept at constant temperature by flowing temperature-controlled water between it and the outer acrylic sleeve (12), serves as the outer block. Argon gas is circulated through the chamber outside of the calorimeter.

2.2. Measurement

The outer active layer is stimulated by sending pulses through the outer layer or layers and returning electrically through the innermost layer. The nature of the pulses is such that its current travels primarily on the surface of the metal in contact with the ceramic (the “skin effect”). This effect is caused by the very fast rise time of the pulses. An

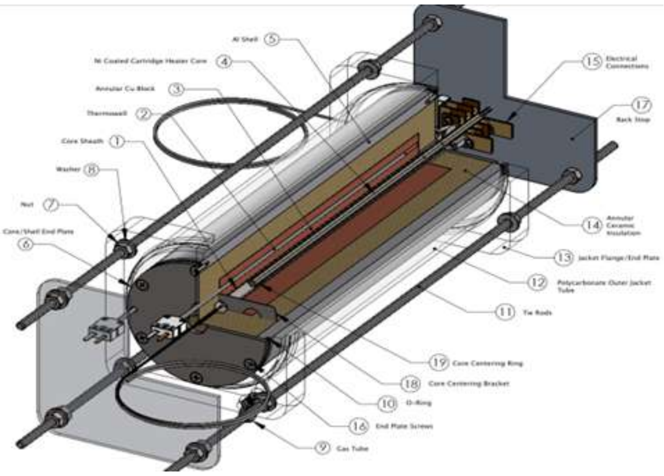

Figure 3. Schematic diagram of the isoperibolic hydrogen hot tube reactor/calorimeter.

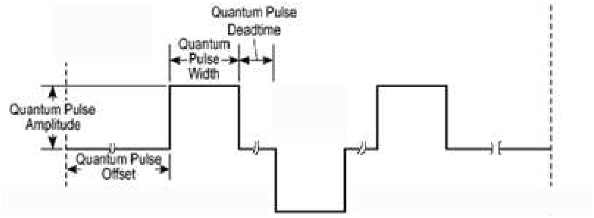

Figure 4. Example of Brillouin's "Q-Pulse".

example of this pulse design, which Brillouin refers to as a "Q-Pulse", is shown in Fig. 4. The pulse width is from $\sim$80 to 1000 ns with a duty cycle of less than 1%. This example shows a pair of pulses with alternating polarity, although same-polarity pulse trains have also been used.

The stimulation power imparted to the core is measured using a circuit shown in Fig. 5. The pulse is generated by a proprietary Q-Pulse board and delivered to the core using series and termination resistors that help match the load impedance to that of the pulse board output. Using a high-speed oscilloscope, the voltage across the end of the core nearest the pulse board is measured as well as the voltage across the opposite end of the core across the termination resistor ($Z_{\rm term}$). The $Z_{\rm term}$ also acts as a current measuring resistor so the current is calculated as $V_2/Z_{\rm term}$. The root mean square (rms) voltage across the $Z_{\rm term}$ is then converted to the rms current.

The voltage across the core is determined using the method shown in Fig. 6. Figure 6a shows the two voltage traces being aligned in a way that minimizes the time difference. This overestimates the power imparted to the core since any phase lag between voltage and current would impart less input power. This voltage difference is shown in the upper plot of Fig. 6b. The current is shown in the middle graph, and the product of these two (power) is shown in the lower plot. It has been shown that the power calculation is essentially the same (within measurement error) whether it is calculated by multiplying the current and voltage plots point by point or by multiplying the calculated rms voltage by the rms current.

In compensation calorimetry, the heater power is varied to keep the core at constant temperature, which generally keeps the inner block at a constant temperature. The difference between the heater power with and without stimulation determines the effect of the stimulation. If this difference is greater than the stimulation that reaches the core, then energy is being produced in the core. Approximately 50 different parameters are collected allowing for calculation of reaction power (the power produced by the process induced by the pulse stimulation). Several calculation methods are possible from these parameters. In Section 2.4, we describe the two methods used.

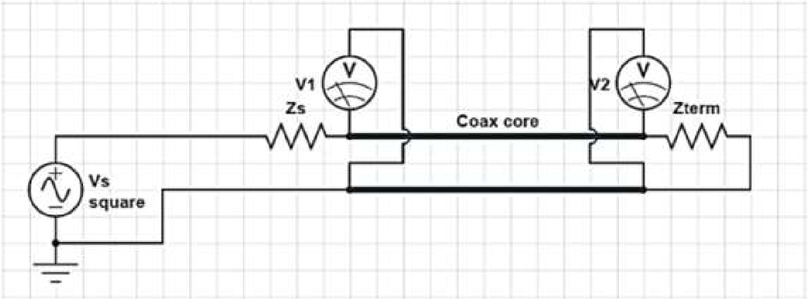

Figure 5. Pulse power measurement circuit.

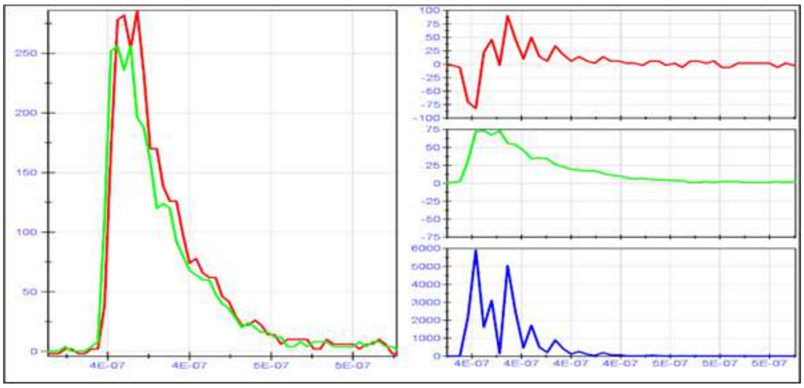

Figure 6. Measurement of the pulse power drop across the core: (a) V_1 and V_2 traces; (b) $V_1 - V_2$, current and power.

2.3. Operation

Figure 7 shows a screenshot from the specially designed proprietary automation and data collection computer program used to control and collect results from the IPB reactor/calorimeter system. The program has several panes allowing for control of temperature, pressure, pulse voltage, pulse power, pulse width, and pulse repetition rate and gas composition. The program also collects the heater power, the pulse power at the generator (as well as at the core), all temperatures, water flow rates, and gas pressure. The concentration of hydrogen and oxygen in the argon blanket are collected and measured. In all, ~50 different parameters are collected and stored every 10 s. A sequence file can be used to automatically change any or all of these parameters at specified intervals over a multi-day or multi-week period.

The sheath containing the core is operated with a static fill of hydrogen, helium, or argon gas held at constant pressure up to 10 bar. The temperature of the core is held constant using its embedded heater and thermocouple and controlled from 200 to 600°C. The outer block temperature is held at 25°C by constant-temperature water flowing from a Neslab® chiller.

The power emanating from the *Q*-pulse generator board is held constant as chosen by the program's front panel or the sequence file. Generally, the pulse amplitude (voltage) and pulse width are chosen. The repetition rate is adjusted automatically to maintain the chosen pulse power. Only a minor fraction of this power reaches the core as most of it is lost as heat in the electrical components and the transmission line. Of that reduced power, only a portion of it influences the heater power as explained in Section 2.2. The actual pulse power is measured directly using the methodology presented above.

Operating in power compensation mode, the computer keeps the inner core temperature constant at its set point. When power is imparted from the *Q*-pulse, the heater power is reduced to compensate and maintain a constant temperature. Hence, the core temperature and the inner and outer block temperatures are all held constant when using the same core gas.

First operating in He gas, a sequence was operated from 200 to 600°C in 50°C intervals. At each temperature, a given DC power was applied to the coating on the core. This process was then repeated while applying constant power pulses with varying pulse width at each temperature. Finally, both automated sequences were repeated in hydrogen gas.

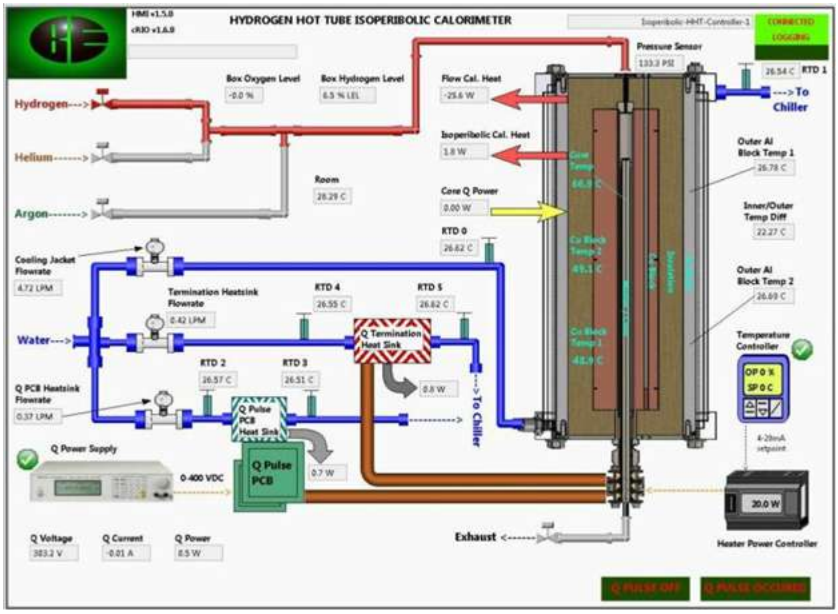

HYDROGEN HOT TUBE ISOPERIBOLIC CALORIMETER

HMI v1.5.0
cRIO v1.6.0
Isoperibolic-HHT-Controller-1

Box Oxygen Level: -0.0 %
Box Hydrogen Level: 0.5 % LEL
Flow Cal. Heat: -25.6 W
Isoperibolic Cal. Heat: 1.8 W
Core Q Power: 0.00 W
Room: 26.29 C
Pressure Sensor: 133.3 PSI
RTD 0: 26.82 C
RTD 1: 26.54 C
RTD 2: 26.57 C
RTD 3: 26.51 C
RTD 4: 26.55 C
RTD 5: 26.82 C
Cooling Jacket Flowrate: 4.72 LPM
Termination Heatsink Flowrate: 0.42 LPM
Q PCB Heatsink Flowrate: 0.37 LPM
Core Temp: 66.9 C
Cu Block Temp 2: 49.1 C
Cu Block Temp 1: 48.9 C
Outer Al Block Temp 1: 26.78 C
Inner/Outer Temp Diff: 22.27 C
Outer Al Block Temp 2: 26.69 C
Temperature Controller: OP 0 % SP 0 C
Heater Power Controller: 20.0 W
Q Voltage: 383.2 V
Q Current: -0.01 A
Q Power: 8.5 W

Figure 7. Screenshot of the automation and data acquisition computer program in operation.

2.4. Analysis

2.4.1. *Method A*

In our IPB design, only a fraction of the stimulation power is imparted to the core heater control because the heater/thermocouple combination is only in contact with approximately half of the core's length. The actual fraction imparted to the core is determined by resistively heating the core's coatings using different powers sourced from a well-measured DC power supply and measuring the heater's response at different temperatures. At each temperature, a linear function ($P_{\text{drop}} = mP_{\text{coating}} + b$) is determined between the power imparted to the core's coating via resistive heating and the power reduction in the internal heater necessary to maintain temperature. Representative linear coefficients at different temperatures are shown in Table 1 and represent the input power lost to the environment.

Table 1. Correlation of power imparted to the core's internal heater by resistively heating its coating: ($P_{\text{drop}} = mP_{\text{coating}} + b$).

Temperature (°C)	m	b
150	0.41	0.07
200	0.44	0.10
250	0.48	0.07
300	0.51	0.06
350	0.55	0.01
400	0.56	0.03
450	0.57	0.03
500	0.57	0.07

The basic calorimetric calculations are shown in Eqs. (1)–(4) when the isoperibolic calorimeter operates in heat flow mode. Heat flow (Q_{flow}) is measured using k_{flow}, which is determined via calibration and the temperature difference between the inner and outer blocks. Heat loss (Q_{loss}) represents the heat loss to air that is not accounted for in (Q_{flow}) and is also determined via calibration. The output heat (Q_{out}) is the sum of (Q_{flow}) and (Q_{loss}). The input heat is the sum of power applied to the heater (Q_{heater}) and the amount of heat experienced by the heater from the pulse (Q_{pulse}). Hence the heat due to the reaction (Q_{reaction}) is the difference between the output and input heats.

$$Q_{\text{reaction}} = Q_{\text{flow}} + Q_{\text{loss}} - (Q_{\text{heater}} + Q_{\text{pulse}}), \tag{1}$$

$$Q_{\text{flow}} = k_{\text{flow}}(T_{\text{core}} - T_{\text{outer}}), \tag{2}$$

$$Q_{\text{loss}} = k_{\text{loss}}(T_{\text{core}} - T_{\text{air}}), \tag{3}$$

$$Q_{\text{out}} = Q_{\text{flow}} + Q_{\text{loss}}. \tag{4}$$

We use the subscripts to mean operation without Q power and operation with Q power. In power compensation mode, we compare the heater power imparted to the core with and without Q pulses applied. Because $T_{\text{core}}, T_{\text{outer}},$ and T_{air} are held constant in this mode, Q_{flow} and Q_{loss} are the same with and without Q power. As such, Eq. (4) cannot be used to calculate Q_{out} in power compensation mode. The difference between $Q_{\text{reaction1}}$ and $Q_{\text{reaction2}}$ is shown in Eq. (5). When Q pulses are not applied, Eq. (6) defines Q_{pulse} and Q_{pulse} to be zero. This simplifies Eq. (5) to that shown in Eq. (7), where ΔQ_{heater} is the difference between the heater applied with and without Q pulses and ΔQ_{out} is output power with and without Q power. The empirical determination of ΔQ_{out} is shown in Eqs. (8)–(10).

$$Q_{\text{reaction2}} - Q_{\text{reaction1}} = (Q_{\text{flow2}} - Q_{\text{flow1}}) + (Q_{\text{loss2}} - Q_{\text{loss1}}) - (Q_{\text{heater2}} - Q_{\text{heater1}}) - (Q_{\text{pulse2}} - Q_{\text{pulse1}}). \tag{5}$$

Without Q pulse:

$$Q_{\text{pulse1}} = Q_{\text{reaction1}} = 0\ \text{W}, \tag{6}$$

$$Q_{\text{reaction}} = (Q_{\text{heater1}} - Q_{\text{heater2}}) = \Delta Q_{\text{heater}} - Q_{\text{pulse}} + \Delta Q_{\text{out}}. \tag{7}$$

Replacing pulses with DC power through the core to emulate the physical source of the heat, as described in the measurement subsection, allows us to determine the amount of Q-pulse power that affects the core heater power when $Q_{\text{reaction}} = 0$. Rearranging Eq. (7) where Q_{heaterDC} is the heater power when DC power is applied to the core coating, Eq. (8) allows us to calculate ΔQ_{out} at different applied DC powers (Q_{DC}). Finding the linear fit parameters from the plot of ΔQ_{out} vs Q_{DC}, Eq. (9) shows us the relationship between applied DC power (Q_{DC}) and the DC power output to the environment (ΔQ_{out}), which cannot be measured directly.

The same equation can be used to find ΔQ_{out} with Q power applied substituting (Q_{pulse}) for Q_{DC}.

$$\Delta Q_{\text{out}} = Q_{\text{DC}} - (Q_{\text{heater}} - Q_{\text{heaterDC}}). \tag{8}$$

Since

$$\Delta Q_{\text{out}} = m(Q_{\text{DC}}) + b \quad \text{then} \quad \Delta Q_{\text{out}} = m(Q_{\text{pulse}}) + b. \tag{9}$$

Equation (10) shows the calculation of Q_{reaction} when operating in power compensation mode where $\Delta Q_{\text{heater}} + \Delta Q_{\text{out}}$ would equal Q_{pulse} (or Q_{DC}) when $Q_{\text{reaction}} = 0$. Equation (11) defines our effective coefficient of performance for the power compensation mode for our isoperibolic calorimeter system.

$$Q_{\text{reaction}} = \Delta Q_{\text{heater}} - Q_{\text{pulse}} + \Delta Q_{\text{out}}, \tag{10}$$

$$\text{COP} = (\Delta Q_{\text{heater}} + \Delta Q_{\text{out}})/Q_{\text{pulse}} = (\Delta Q_{\text{heater}} + m(Q_{\text{pulse}}) + b)/Q_{\text{pulse}}. \tag{11}$$

2.4.2. *Method B*

The second method of analyzing the calorimetry is more direct; instead of calculating the power loss by the calorimeter, it determines the amount of heater power compensation (HPC) for different amounts of DC calibration power P_{DC} at different temperatures. In fact, this method is analogous to the traditional isoperibolic calorimeter analysis except that it substitutes heater power compensation for the temperature difference, i.e. the calibration curve at each temperature is determined by plotting HPC versus P_{DC}. In order to calculate Q_{reaction}, Method B compares the HPC from the Q pulse experiment to the HPC vs. P_{DC} calibration curve at the same temperature. Using this DC calibration, the relationship between input power and HPC is determined so that with input pulse power the HPC can be used to back-calculate the power from the pulse imparted into the core.

First, the linear relationship between HPC and DC power (P_{DC}) is found by fitting a linear equation to HPC vs. P_{DC} when P_{DC} is varied across the range of Q_{pulse} powers. These linear coefficients (M) are then applied to the HPC measured during Q_{pulse} stimulation HPC(Q) to calculate delta output power (ΔP_{out}) = HPC(Q)/M. Q_{reaction} is then calculated as shown in Eq. (12), where HPC(Q) is the actual HPC measured when the pulse is applied. Equation (13) is then used to calculate the coefficient of performance (COP). Alternatively, stimulated power gain (SPG) can be calculated as shown in Eq. (14).

$$Q_{\text{reaction}} = \text{HPC}(Q) - \text{HPC(DC)}, \tag{12}$$

$$\text{COP} = Q_{\text{reaction}}/Q_{\text{pulse}} = (\text{HPC}(Q) - \text{HPC(DC)})/Q_{\text{pulse}}, \tag{13}$$

$$\text{SPG} = \Delta P_{\text{out}}/Q_{\text{pulse}}.$$

Table 2. List of linear fit coefficients determined and employed in Method B.

Temperature (°C)	M
150	0.45
200	0.47
250	0.50
300	0.53
350	0.57
400	0.58

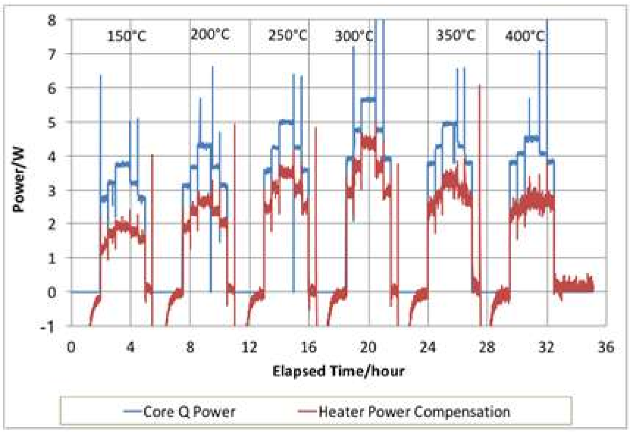

Figure 8. Plot of Q pulse power and heater power compensation at constant temperatures from 150 to 400°C.

The linear slope coefficient is similar to the value "m" used in Method A, which uses the fit to determine the input power lost to the environment. Method B uses the fit to determine the percentage of input power that interacts with the core's heater and thermocouple. Table 2 shows the values for "M", the linear fit coefficient from Method B.

3. Results and Discussion

The pulse width was varied from 100 to 300 ns and back to 100 ns while maintaining constant Q power and constant temperature. This was repeated at five different temperatures (held constant) from 150 to 400°C. The reduction in heater power (heater power compensation, HPC) is equal to the Q pulse power that reaches the heater plus Q_{reaction}. Figure 8 shows HPC and Q pulse power at these temperatures while varying the pulse width.

Note that the power compensation amount is very dependent on the pulse length at 300°C. Although the total pulse power from the generator is constant, the pulse power measured at the core does vary with pulse length. Still, the

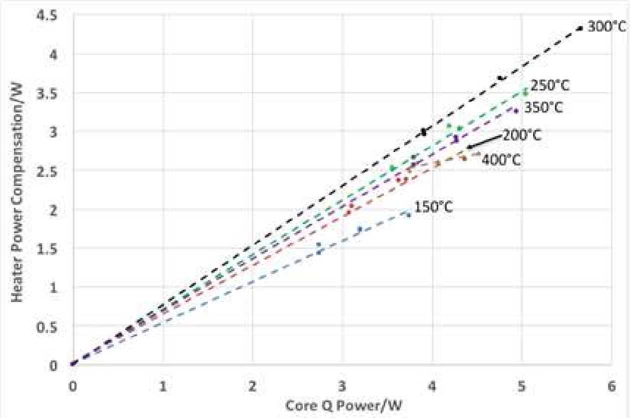

Figure 9. Plot of heater power compensation vs. Q pulse power from 150 to 400°C.

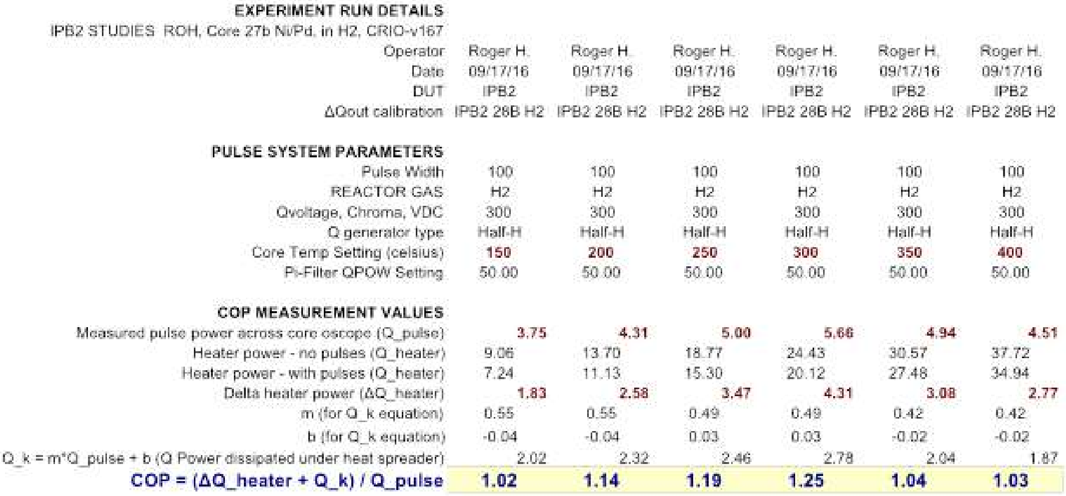

EXPERIMENT RUN DETAILS						
IPB2 STUDIES ROH, Core 27b Ni/Pd, in H2, CRIO-v167						
Operator	Roger H.	Roger H.	Roger H.	Roger H.	Roger H.	Roger H.
Date	09/17/16	09/17/16	09/17/16	09/17/16	09/17/16	09/17/16
DUT	IPB2	IPB2	IPB2	IPB2	IPB2	IPB2
ΔQout calibration	IPB2 28B H2	IPB2 28B H2	IPB2 28B H2	IPB2 28B H2	IPB2 28B H2	IPB2 28B H2
PULSE SYSTEM PARAMETERS						
Pulse Width	100	100	100	100	100	100
REACTOR GAS	H2	H2	H2	H2	H2	H2
Qvoltage, Chroma, VDC	300	300	300	300	300	300
Q generator type	Half-H	Half-H	Half-H	Half-H	Half-H	Half-H
Core Temp Setting (celsius)	**150**	**200**	**250**	**300**	**350**	**400**
Pi-Filter QPOW Setting	50.00	50.00	50.00	50.00	50.00	50.00
COP MEASUREMENT VALUES						
Measured pulse power across core oscope (Q_pulse)	**3.75**	**4.31**	**5.00**	**5.66**	**4.94**	**4.51**
Heater power - no pulses (Q_heater)	9.06	13.70	18.77	24.43	30.57	37.72
Heater power - with pulses (Q_heater)	7.24	11.13	15.30	20.12	27.48	34.94
Delta heater power (ΔQ_heater)	**1.83**	**2.58**	**3.47**	**4.31**	**3.08**	**2.77**
m (for Q_k equation)	0.55	0.55	0.49	0.49	0.42	0.42
b (for Q_k equation)	-0.04	-0.04	0.03	0.03	-0.02	-0.02
Q_k = m*Q_pulse + b (Q Power dissipated under heat spreader)	2.02	2.32	2.46	2.78	2.04	1.87
COP = (ΔQ_heater + Q_k) / Q_pulse	**1.02**	**1.14**	**1.19**	**1.25**	**1.04**	**1.03**

Figure 10. Summary of COP calculations from a Q-pulse length run similar to that shown in Fig. 9.

magnitude of the power compensation is a greater percentage of the pulse power at 100 ns than at 300 ns. Calculations show that at 300 ns, the Q_{reaction} is quite small but is of much greater magnitude at 100 ns. Figure 9 shows the effect of temperature on HPC versus pulse power at different temperatures. The summary of the COP results from the data shown in Figs. 8 and 9 calculated using Method A is shown in Fig. 10. Table 3 summarizes the COP results from six such runs.

It is important to note in Table 3 that the runs performed at 300°C showed COP significantly greater than 1.0, while those at 600°C were essentially 1.0 within experimental error. This may be explained as the Pd inner layer totally deloading its hydrogen as we have seen before at this temperature and the Ni, although retaining hydrogen traverses its Curie point, changing its electrical and chemical properties. Similar results have been seen from more than 50 runs performed over this period.

Method B was used to calculate COP from some more recent runs similar to that shown in Figs. 8 and 9. As shown above, operating above 600°C usually does not yield any reaction heat. Recent runs were operated only up to 400°C. Table 4 summarizes the Q_{reaction} and SPG calculated from recent runs analyzed using Method B.

There are many more test runs that occurred with Brillouin's IPB hydrogen hot tubes (HHTs), which can be

Table 3. Summary of COP calculations from six Q-pulse runs similar to that shown in Figs. 8 and 9 up to 600°C.

Temperature (°C)	Pulse width (ns)	COP	Error ±
300	150	1.4	0.1
250	150	1.4	0.1
300	150	1.2	0.1
600	150	1.0	0.1
300	300	1.3	0.1
600	150	1.01	0.08
300	150	1.4	0.1

Table 4. Q_{reaction} and SPG from recent runs calculated using Method B.

Temperature (°C)	Q_{reaction} at 100 ns (W)	Q_{reaction} at 150 ns (W)	Error ± (W)	SPG at 100 ns	SPG at 150 ns
150	0.73	0.88	0.08	1.2	1.3
200	0.99	1.15	0.08	1.3	1.4
250	1.18	1.5	0.1	1.3	1.5
300	1.9	2.1	0.2	1.5	1.6
350	1.4	1.7	0.2	1.4	1.5
400	1.1	1.4	0.1	1.3	1.4

analyzed using these and other methods but the COP's and SPG's found in those tests are very similar to the runs that were examined and summarized herein.

4. Conclusion

LENR can produce thermal power when Ni and other metal-coated tubes are stimulated using fast rise-time pulses. These experiments operated in H_2 or He gas from 200 to 600°C. The exact same procedure was performed in each gas. Comparative thermal measurements were performed between heater-only power and heater and pulse power.

These runs were performed in isoperibolic calorimeters operated in power-compensation mode, where the heater adjusts its power to keep the inner and outer temperature difference constant. Over 100 runs were performed on five different Ni-coated cores. Three additional cores were also tested for other experimental purposes. Stimulated power gain values from 1.0 to over 2.0 were measured depending on stimulation conditions. It is important to note that these calculations ignore the heater power necessary to maintain temperature, which can be several times greater than either the stimulation power or power gain. Recent test runs have not averaged above 1.5, although the core's coating composition and metallurgy are still being optimized. The calorimetry is still being optimized. The COP and SPG results presented here ignore the heater power necessary to maintain temperature, and the electrical losses in the pulse generator, both of which can be several times greater than either the stimulation power or power gain.

Acknowledgements

I would like to acknowledge Dr. Michael McKubre (SRI Emeritus) for his work on the calorimeter design and thank Brillouin Energy scientists Jin Liu, Roger Tong and Mark Garnett for their aid in the calorimetric analysis. I also acknowledge the Brillouin Energy Corp. for their generous support of this work.

References

[1] R. Godes, R. George, F. Tanzella and M. McKubre, *J. Condensed Matter Nucl. Sci.* **13** (2015) 127.
[2] R. Godes, Drive circuit and method for semiconductor devices, US Patent 8,624,636, 2014.